Received: 2 August 2021 | Revised: 26 October 2021 | Accepted: 14 November 2021

IET Renewable Power Generation

DOI: 10.1049/rpg2.12350

The Institution of Engineering and Technology WILEY

ORIGINAL RESEARCH PAPER

Voltage control method based on three-phase four-wire sensitivity for hybrid AC/DC low-voltage distribution networks with high-penetration PVs

Lu Zhang[1] | **Chunxue Zhao**[1] | **Bo Zhang**[1] | **Gen Li**[2] | **Wei Tang**[1]

[1] College of Information and Electrical Engineering, China Agricultural University, Beijing, China

[2] School of Engineering, Cardiff University, Cardiff, UK

Correspondence
Wei Tang, College of Information and Electrical Engineering, China Agricultural University, Beijing 100083, China.
Email: wei_tang@cau.edu.cn

Funding information
National Key Research and Development Program of China, Grant/Award Number: 2019YFE0118400

Abstract

The increasing integration of distributed photovoltaics may further aggravate the over-voltage and three-phase unbalance issues of low-voltage distribution networks with three-phase four-wire structures. The voltage control method based on the AC and DC side power flow control and the three-phase power control capability of voltage source converter in hybrid AC/DC low-voltage distribution networks is a solution for the improvement of the above power quality issues. In this paper, an accurately improved sensitivity matrix calculation method considering shunt admittance based on the ABCD parameters is proposed in hybrid AC/DC low-voltage distribution networks with a three-phase four-wire structure. The presented ABCD parameters of the feeders consider the influence of the coupling effect among phases and the neutral line on sensitivity calculation, which makes the sensitivity calculation simple. Then, a power-voltage control method for voltage source converters based on three-phase four-wire sensitivity matrices of the AC side is proposed considering the constraints from the voltage source converter and DC side power flow in hybrid AC/DC low-voltage distribution networks, which can effectively address the over-voltage and unbalanced issues. Simulations are performed to verify the proposed sensitivity calculation method and voltage control method.

1 | INTRODUCTION

The use of renewable energy resources, such as wind and solar power, is the main solution to achieve the net-zero emission [1]. However, the integration of single-phase grid-connection photovoltaics (PVs) may exacerbate the three-phase unbalance issues in the low-voltage distribution networks (LVDNs) with the three-phase four-wire structure [2]. Moreover, the mismatch between the generation and demand of PVs and loads may lead to over-voltages in LVDNs [3]. The high penetration of PVs makes it more difficult to address the power quality problems of LVDNs. Therefore, it is of great significance to study the power quality management of three-phase four-wire LVDNs.

Various measures have been proposed to manage power quality. Traditional power quality control equipment, such as shunt capacitors and phase change switches, cannot operate frequently and have limited control ability [4]. Static var generator (SVG), PV inverter [5] and other power electronics devices have flexible power regulation ability, which can mitigate the over-voltage and three-phase unbalance problems of LVDNs. However, these devices cannot break the bottleneck of radial operation of distribution networks. Distribution network equipped with soft open points (SOP) can connect two AC lines to achieve the loop operation [6], which realises the flexible power scheduling of the network by controlling the converters on both sides [7]. However, the installation of SOP cannot enhance the power supply capacity of the distribution networks.

The DC technology features in high power transfer capability and converter flexible control, which complements the conventional AC by forming hybrid AC/DC systems. The AC/DC LVDN is more functional and controllable than AC LVDN. For instance, an AC/DC LVDN can mitigate overload and node voltage violation issues due to the high-power transfer capacity

of DC lines as well as the capability of power flow rescheduling in AC/DC LVDN, in which the bottleneck of radial operation of AC LVDN can be broken [8, 9]. Moreover, the unbalanced issues in LVDN can also be mitigated by the single-phase control of converters [7]. Hybrid AC/DC LVDNs have been designed and implemented in several real applications (e.g. the Tangjia Bay DC Distribution Pilot Project and Hangzhou Dajiangdong Project) [10–12] which demonstrate the merits of using the AC/DC LVDN technology.

AC LVDNs commonly use the three-phase four-wire structure, in which loads and PVs are connected in single-phase between the neutral wire. Such structure faces the over-voltage and three-phase unbalance issues, which are exacerbated due to the increasing unbalanced distribution of distributed generation (e.g. PV). In [13], a flexible day-ahead optimal control model is developed based on the three-phase sensitivity approaches to solve the over-voltage problems and alleviate the neutral voltage rise in three-phase four-wire AC LVDNs. Reference [14] proposes an optimal local reactive power control of single-phase inverters to improve the voltage unbalance issues in three-phase four-wire LVDNs. However, the over-voltage and unbalanced issues are not addressed at the same time. Based on the sensitivity theory, [15] proposes a voltage control strategy for the cooperative control of energy storage and on-load tap changers, which solves the over-voltage and unbalanced issues in three-phase four-wire LVDNs. Reference [16] proposes a reactive power regulation of single-phase PV inverter to solve the over-voltage and unbalanced issues in three-phase four-wire LVDNs. However, the coupling effect among phases is not considered in [15] and [16].

Sensitivity methods can quickly obtain core control variables (e.g. node active/reactive power and voltages) which will be used to cope with the frequent voltage regulation for regulating the fluctuations caused by PVs. The condition of calculating the sensitivity based on the Jacobian Matrix is rigorous because the Jacobian Matrix can only be used when the inversion exists [17]. The sensitivity calculation method based on the Newton–Raphson method is not suitable for AC LVDNs, because the radial AC LVDNs generally use the Backward/Forward method for power flow calculation. In [18], a centralised control method base on linear sensitivity is proposed to reduce the number of Backward/Forward substitutions in power flow calculation. However, the three-phase four-wire structure and interphase coupling of AC LVDNs are not studied. Reference [19] calculates the three-phase sensitivity through the series line model without considering the shunt admittance. However, the accuracy of sensitivity is reduced and this method can only be used when the shunt admittance can be ignored by transforming the three-phase four-wire line model into a three-phase three-wire. Reference [20] considers the shunt admittance line model and uses a three-phase admittance matrix to calculate sensitivity. However, the calculation equations are too complicated and therefore, the calculation time is long. The three-phase calculation model also does not consider the influence of the neutral line. The above literatures focus on the voltage control methods to solve the power quality issues and three-phase sensitivity for distribution networks. The sensitivity calculation methods and voltage control methods based on sensitivity to address the over-voltage and unbalanced issues for three-phase four-wire AC LVDNs are still under-researched.

Power control based on VSC can be a voltage regulation method in hybrid AC/DC LVDNs [21]. The power quality problems in hybrid AC/DC LVDNs can be solved by the AC and DC side power flow control and the three-phase power control capability of VSC. Reference [22] proposes an improved method through the zero-sequence voltage injection in the converters to keep balancing the three-phase grid currents and DC capacitor voltages in the DC side. In [23], the hybrid AC/DC microgrid has dealt with the impact of uncertainty on the power interaction by managing the charge/discharge of energy storage. However, research on the control of hybrid AC/DC LVDNs mainly focuses on the local control strategies, the flexible power regulation ability between AC and DC interconnection lines is not fully considered from the whole system perspective of hybrid AC/DC LVDNs. The following aspects would be considered in this paper:

1. The accuracy of the existing sensitivity calculation methods can be further improved when considering the three-phase four-wire structure on the AC side of a hybrid AC/DC LVDN. Moreover, there will be unbalanced current in the neutral line when three phases are unbalanced. Therefore, the three-phase three-wire AC line model established by combining the impedance of the neutral line into the phase-to-phase impedance cannot fully describe the characteristics of the low-voltage AC distribution line. The accuracy of the three-phase three-wire sensitivity is not high because it does not consider the influence of the coupling effect among phases and the influence from the neutral line on the sensitivity calculation.
2. Although the VSC can realise single-phase regulation to solve the power quality problems for each phase, the phase regulation needs to meet the total capacity limit of the VSCs and the power flow constraints of the DC distribution network. If the constraints of VSCs and DC distribution network are not considered comprehensively, the precise control ability of VSCs cannot be fully released.

In order to address the above concerns, a sensitivity matrix calculation method considering the three-phase four-wire grid is proposed. A power-voltage phase control method for VSCs based on three-phase four-wire sensitivity matrix is proposed considering the constraints from the VSCs and DC side power flow. The contributions of this paper are as follows.

1. Generate the ABCD parameter matrices considering the interphase coupling of the lines and the three-phase four-wire grid structure of the AC side of hybrid AC/DC LVDNs. Based on three-phase four-wire ABCD parameters, this paper proposes an improved sensitivity calculation method considering the radial network and three-phase four-wire structure with shunt admittance for hybrid AC/DC LADNs,

which further improve the accuracy of the sensitivity calculation.

2. Propose a voltage control method for hybrid AC/DC LVDNs to address the over-voltage and unbalanced issues, which takes the advantage of the three-phase four-wire sensitivity and considers the constraints of VSC capacity and DC power flow. The sensitivities of AC and DC lines in this paper are decoupled by VSCs because of their flexible control ability of active and reactive power.

2 | IMPROVED SENSITIVITY CALCULATION METHOD

An improved sensitivity calculation method for three-phase unbalanced distribution network on VSC's AC side is proposed in this paper. The sensitivity algorithm does not need iteration. Therefore, there is no convergence problem. This improved sensitivity calculation method depends on the ABCD parameters of the feeders, which only relates to the line configuration and distribution network structure. If the network configuration does not change, the ABCD parameters will be constant. Therefore, the sensitivity calculation method is applicable to the general hybrid AC/DC LVDNs structure. Moreover, the equivalent resistances and reactances can be formed through multipliying the parameters of ABCD parameters of cascaded feeders. This method does not need to update the data in each control step in real-time. It only needs to update the voltage of the nodes, and directly calculates the required hybrid AC/DC LVDNs sensitivity coefficients using the methods derived below. The used VSC control (P-Q and V_{dc}-Q) is typical control strategies which are widely used in real applications. The required adjustment values of active and reactive power of VSCs can be calculated by the proposed sensitivity matrices and then applied in the VSC control.

2.1 | Sensitivity of three-phase four-wire AC LVDNs

2.1.1 | ABCD parameters calculation

The voltage of any node i in the distribution network is expressed as

$$U_i = U_j + \sum_{l \in C_{i,j}} \frac{P_{\mathrm{line},l} R_l + Q_{\mathrm{line},l} X_l}{U_l}, \tag{1}$$

where $C_{i,j}$ is the set of all lines and nodes between nodes i and j. The number of each section of the line is the same as the number of the last node of this line. U_j and U_i are the voltages of nodes j and i. $P_{\mathrm{line},l}$ and $Q_{\mathrm{line},l}$ are the active and reactive power of the power distribution line between nodes l-1 and l. R_l and X_l are the equivalent resistance and reactance of the power distribution line between nodes l-1 and l.

The voltage sensitivities at node j due to the injected active and reactive power at node i are:

$$S_{j,i}^{U-P} = \frac{\partial U_j}{\partial P_i} \approx -\sum_{l \in (C_{0,i} \cap C_{0,j})} \frac{R_l}{U_l}, \tag{2}$$

$$S_{j,i}^{U-Q} = \frac{\partial U_j}{\partial Q_i} \approx -\sum_{l \in (C_{0,i} \cap C_{0,j})} \frac{X_l}{U_l}. \tag{3}$$

For the three-phase four-wire network, the π-section line model containing the line-to-ground admittance and line mutual impedance is used. A line model between the nodes m and n is shown in Figure 1. The first node of the line is set as the reference node whose voltage is U_0. Loads are connected to the nodes m and n.

Based on Kirchhoff's Current and Voltage Laws, the input voltage and the current of node m in the π-section line model have the following relationship:

$$\begin{bmatrix} U_m^{\varphi} \\ I_m^{\varphi} \end{bmatrix} = \begin{bmatrix} a & b \\ c & d \end{bmatrix} \begin{bmatrix} U_n^{\varphi} \\ I_n^{\varphi} \end{bmatrix}, \tag{4}$$

where

$$\begin{aligned} a &= X + 1/2ZY \\ b &= Z \\ c &= Y + 1/4YZY, \\ d &= X + 1/2ZY \end{aligned} \tag{5}$$

where U_m^{φ} and U_n^{φ} are the input and output voltages of nodes m and n. I_m^{φ} and I_n^{φ} are the input and output currents of π-section line model between nodes m and n, as shown in Figure 1. φ is the set of phases a, b, c and neutral phase n. The size of the a, b, c, d and X, Y, Z matrices is 4×4. X, Y, Z are the identity matrix, shunt admittance matrix and line impedance matrix.

According to Kirchhoff's Current Law, the currents in the line model satisfy the following equations:

$$\begin{bmatrix} I_n^a \\ I_n^b \\ I_n^c \\ I_n^n \end{bmatrix} = \begin{bmatrix} I_n^{a\prime} + I_{\mathrm{load},n}^a \\ I_n^{b\prime} + I_{\mathrm{load},n}^b \\ I_n^{c\prime} + I_{\mathrm{load},n}^c \\ I_n^{n\prime} - I_{\mathrm{load},n}^a - I_{\mathrm{load},n}^b - I_{\mathrm{load},n}^c \end{bmatrix}, \tag{6}$$

$$\begin{bmatrix} I_m^a \\ I_m^b \\ I_m^c \\ I_m^n \end{bmatrix} = \begin{bmatrix} I_m^{a\prime} - I_{\mathrm{load,m}}^a \\ I_m^{b\prime} - I_{\mathrm{load,m}}^b \\ I_m^{c\prime} - I_{\mathrm{load,m}}^c \\ I_m^{n\prime} + I_{\mathrm{load,m}}^a + I_{\mathrm{load,m}}^b + I_{\mathrm{load,m}}^c \end{bmatrix}, \tag{7}$$

where I_m^{φ} and $I_n^{\varphi\prime}$ are the input and output currents of nodes m and n, as shown in Figure 1. $I_{\mathrm{load,m}}^{\varphi}$ and $I_{\mathrm{load,n}}^{\varphi}$ are the load currents of phase φ of nodes m and n. The load connected to the neutral line is zero.

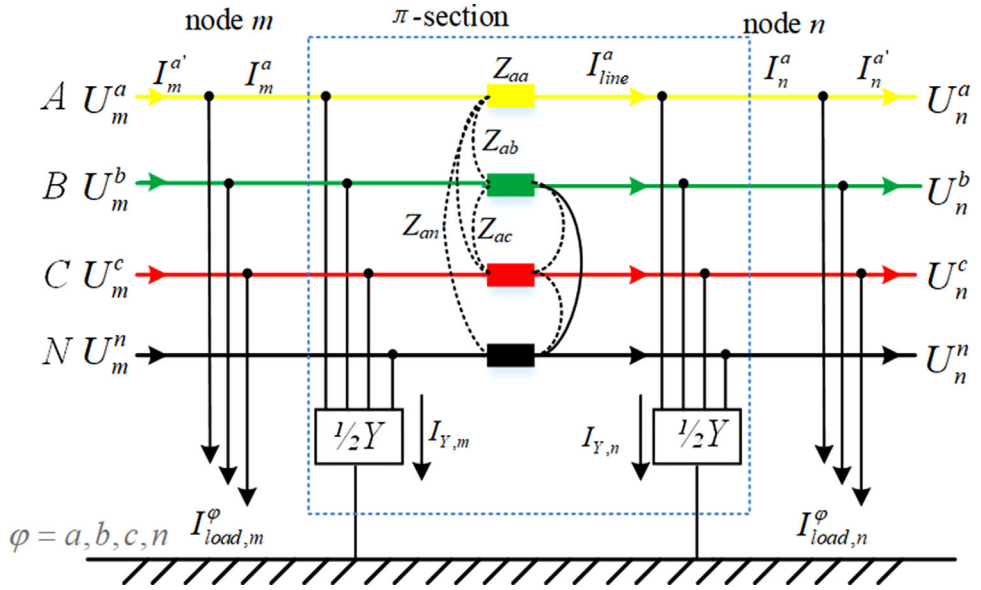

FIGURE 1 Model of the three-phase four-wire distribution network

Equation (4) can also be converted to calculate the voltage of the node n by using the voltage of node m:

$$U_n^{\varphi} = AU_m^{\varphi} - BI_n^{\varphi}, \tag{8}$$

where $A = a^{-1}$ and $B = a^{-1}b$.

The ABCD parameters can be obtained through recursively multiplying the *abcd* parameters of all components from the path between two nodes in order. Therefore, the equivalent ABCD parameters between nodes i and j is

$$\begin{bmatrix} a_{ij} & b_{ij} \\ c_{ij} & d_{ij} \end{bmatrix} = \prod_{l \in C_{i,j}} \begin{bmatrix} a_l & b_l \\ c_l & d_l \end{bmatrix}. \tag{9}$$

For ease of reading, the subscripts of the *abcd* parameters between the power source and other node are simplified to the value of the other node, for example a_j represents the parameter of the power source and the node j.

According to Equation (8), it can be obtained

$$U_j^{\varphi} = A_j U_0^{\varphi} - B_j I_j^{\varphi}, \tag{10}$$

where $A_j = a_j^{-1}$ and $B_j = a_j^{-1} b_j$.

2.1.2 | Three-phase four-wire sensitivity calculation

The power-voltage sensitivity can be obtained by calculating the derivative of Equation (10) with respect to power (P):

$$\frac{\partial U_j^{\varphi}}{\partial P_i^{\varphi}} = -\frac{1}{U_i^{\varphi}} \mathrm{Re}\left(\frac{\partial B_j I_j^{\varphi}}{\partial I_{\mathrm{load},i}^{\varphi}} \right), \tag{11}$$

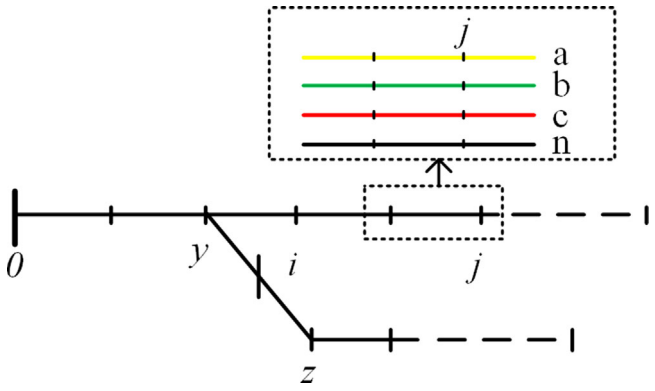

FIGURE 2 Low-voltage radial distribution network.

$$\frac{\partial U_j^{\varphi}}{\partial Q_i^{\varphi}} = -\frac{1}{U_i^{\varphi}} \mathrm{Im}\left(\frac{\partial B_j I_j^{\varphi}}{\partial I_{\mathrm{load},i}^{\varphi}} \right). \tag{12}$$

The equivalent resistance and reactance in Equations (2) and (3) can be replaced by the ABCD parameters considering the structure of the three-phase four-wire AC LVDNs. Then, the three-phase four-wire sensitivity calculation formula based on ABCD parameters can be obtained.

A radial AC LVDNs structure shown in Figure 2 is considered. The position and phase of the nodes will affect the sensitivity calculation. x ($x \in \{a, b, c, n\}$) and v ($v \in \{a, b, c, n\}$) ($x \neq v$) are used to describe the phases of the two selected nodes. The three-phase four-wire sensitivity calculation is discussed in the following two aspects.

(a) Voltage sensitivity between phases at the same node

If the reactive power source is connected to phase x of node j and is used to control phase v of node j, then the equivalent

resistance and reactance will be

$$\sum R_l = \mathrm{Re}\left(\left[B_j\right]_{v,\varkappa}\right), \tag{13}$$

$$\sum X_l = \mathrm{Im}\left(\left[B_j\right]_{v,\varkappa}\right), \tag{14}$$

where the notation $[B]_{v,\varkappa}$ is the element in row v and column $\varkappa$ of matrix B.

(b) Voltage Sensitivity between different nodes

When the voltage controlled node is not the node where the power changes, the sensitivity is calculated in the following three cases.

Case 1: The voltage sensitivities at node j due to the injected power at node i. The two nodes are in the same line.

If the power source is connected to phase v of node i and is used to control the voltage of phase $\varkappa$ of node j, then the equivalent resistance and reactance are

$$\sum R_l = \mathrm{Re}\left[A_{ij}\left[B_j\right]_{\varkappa\varkappa}\right]_{rv}, \tag{15}$$

$$\sum X_l = \mathrm{Im}\left[A_{ij}\left[B_j\right]_{\varkappa\varkappa}\right]_{rv}, \tag{16}$$

where $[B_j]_{\varkappa\varkappa}$ is the element in column $\varkappa$ of matrix B_j and $[B_j]_{rv}$ is the element in row v of matrix B_j.

Case 2: The voltage sensitivities at node i due to the injected power at node j. The two nodes are in the same line.

If the power source is connected to phase v of node j and is used to control the voltage of phase $\varkappa$ of node i, then the equivalent resistance and reactance are

$$\sum R_l = \mathrm{Re}\left[a_{ij}\left[B_j\right]_{\varkappa\varkappa} + \left[B_{ij}\right]_{\varkappa\varkappa}\right]_{rv}, \tag{17}$$

$$\sum X_l = \mathrm{Im}\left[a_{ij}\left[B_j\right]_{\varkappa\varkappa} + \left[B_{ij}\right]_{\varkappa\varkappa}\right]_{rv}. \tag{18}$$

Case 3: The voltage sensitivities at node z due to the injected power at node j. The two nodes are in different lines.

If the power source is connected to phase v of node j and is used to control the voltage of phase $\varkappa$ of node z, then the equivalent resistance and reactance are

$$\sum R_l = \mathrm{Re}\left[A_{yz}\left(a_{yj}\left[B_j\right]_{\varkappa\varkappa} + \left[b_{yj}\right]_{\varkappa\varkappa}\right)\right]_{rv}, \tag{19}$$

$$\sum X_l = \mathrm{Im}\left[A_{yz}\left(a_{yj}\left[B_j\right]_{\varkappa\varkappa} + \left[b_{yj}\right]_{\varkappa\varkappa}\right)\right]_{rv}. \tag{20}$$

As long as the network configuration is constant, $\sum R_l$ and $\sum X_l$ are constant. Once they are obtained, they will be stored in the controller. The sensitivity value will only be updated by Equations (2) and (3) when the voltage changes.

2.2 | Augmented sensitivity matrix of hybrid AC/DC LVDNs

The ABCD parameters calculation method is also applicable to the DC distribution network. When calculating the sensitivity of the positive and negative poles of the DC side, the inductance and capacitance of the DC line will be set as zero. The sensitivities of AC and DC lines in this paper are decoupled by VSCs because of their control ability of active and reactive power.

Based on ABCD parameters, the power-voltage sensitivities of the AC side and DC side LVDNs are calculated. Then, a power-voltage augmented sensitivity matrix containing all nodes of the hybrid AC/DC LVDNs can be obtained:

$$S = \begin{bmatrix} SAC^{U-P} & SAC^{U-Q} \\ SDC^{U-P} & SDC^{U-Q} \end{bmatrix}, \tag{21}$$

where $SAC^{U\text{-}P}$ and $SAC^{U\text{-}Q}$ are the active power-voltage sensitivity and reactive power-voltage sensitivity matrices of AC side distribution network. $SDC^{U\text{-}P}$ and $SDC^{U\text{-}Q}$ are the active power-voltage sensitivity and reactive power-voltage sensitivity matrices of DC side distribution network, respectively.

3 | VOLTAGE CONTROL

The node voltage is related to both active and reactive power in hybrid AC/DC LVDNs. It is because the ratio of R/X in LVDNs is higher than that in the high voltage transmission networks. In this section, different voltage control methods aiming at alleviating the over-voltage and three-phase unbalance are presented, which are based on the modified three-phase four-wire sensitivity proposed in Section 2. Moreover, a power-voltage control strategy based on the separate phase-control ability of VSC is proposed considering the concurrent power quality issues in hybrid AC/DC LVDNs.

3.1 | Hybrid AC/DC LVDNs

A typical hybrid AC/DC LVDNs is shown in Figure 3. The AC side is three-phase four-wire. The DC side is symmetrical monopole with metallic return. The DC voltage is ±375 V. There are DC loads in the DC side.

VSC can simultaneously control any two state quantities of DC voltage, AC voltage, active power and reactive power [24]. Therefore, VSC has V_{dc}-Q, P-Q, V_{dc}-U_{ac} and other control modes [25]. VSC1 is in the V_{dc}-Q control mode to control the DC voltage, and VSC2 is in the P-Q control mode which the sensitivity calculation method proposed in this paper is appropriate to. Through active and reactive power control of VSC2, the power transfer between interconnected lines can be realised, so as to alleviate the over-voltage and three-phase unbalance issues.

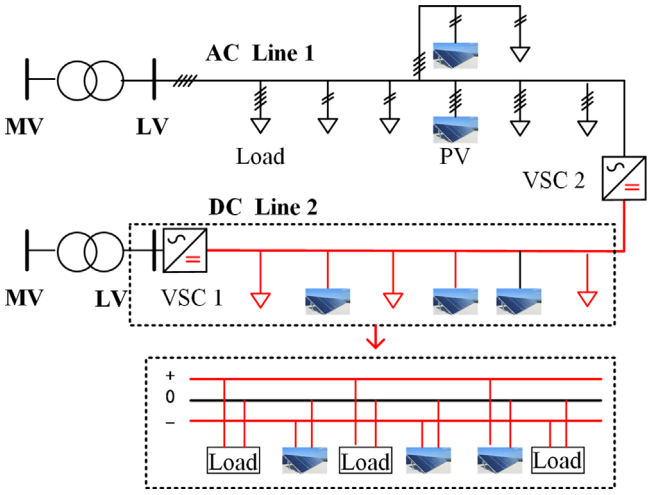

FIGURE 3 Hybrid AC/DC LVDNs

3.2 | Power control strategy based on power-voltage sensitivity

If the three-phase unbalance issue on the AC side is considered firstly, adjusting the voltage unbalance factor (VUF) may lead to over-voltage at the phases with normal voltage. Therefore, the over-voltage will be solved firstly and then alleviate the three-phase unbalance problem.

The constraints of VSCs and DC distribution network will be fully considered in the voltage control method as shown in Figure 4.

The voltage control methods for alleviating over-voltage and solving three-phase unbalance problems are presented as follow.

(a) Alleviation of the over-voltage problems.

The total active power of VSC2 on the AC side and DC side should meet the constraint of VSC2's capacity:

$$\begin{cases} \left|P_{VSC2}^{AC}\right| = \left|P_{VSC2}^{DC}\right| + P_{VSC2,\text{loss}} \\ P_{VSC2}^{AC2} + Q_{VSC2}^{AC2} = S_{VSC2,\max}{}^2 \end{cases}, \tag{22}$$

where P_{VSC2}^{AC} and P_{VSC2}^{DC} are the active power of VSC2 on the AC side and DC side, Q_{VSC2}^{AC} is the reactive power of VSC2, $S_{VSC2,\max}$ is the rated apparent power of VSC2. $P_{VSC2,\text{loss}}$ is the power losses of VSC2, which can be calculated through the following equation and has been used in distribution networks [26, 27].

$$P_{VSC2,\text{loss}} = uI_{DC2}^2 + vI_{DC2} + w, \tag{23}$$

where I_{DC2} is the DC current of the VSC2. u and v are the factors representing the quadratic and linear dependency of converter losses on the converter current. w indicates no-load converter losses. Generally, the power losses of VSCs are around 2% [28] and the power losses calculated from (23) will fall in this range. Therefore, to simplify the calculation of the power losses of VSC2 the following relationship is considered:

$$P_{VSC2,\text{loss}} = 0.02P_{VSC2,\text{rate}}, \tag{24}$$

where $P_{VSC2,\text{rate}}$ is the rated active power of VSC2.

If a DC node voltage exceeds the limits, real power will be used to regulate node voltages based on Equation (25).

$$\left[\Delta P_{VSC2}^{DC}\right] = \left[SDC_{VSC2,i}^{U-P}\right]^T \left[\Delta U_i^{DC}\right], \tag{25}$$

where ΔU_i^{DC} is the voltage deviation between the measured voltage and a lower or an upper limit, which is 0.93 p.u. for the under-voltage or 1.07 p.u. for the over-voltage cases respectively. SDC_{VSC2}^{U-P} is the sensitivity of the ratio of the active power of VSC2 and voltage at node i. ΔP_{VSC2}^{DC} is the regulated active power of VSC2 on the AC side.

If the active power adjustment cannot be achieved due to the power rating limit of VSC2, the active capacity will be released

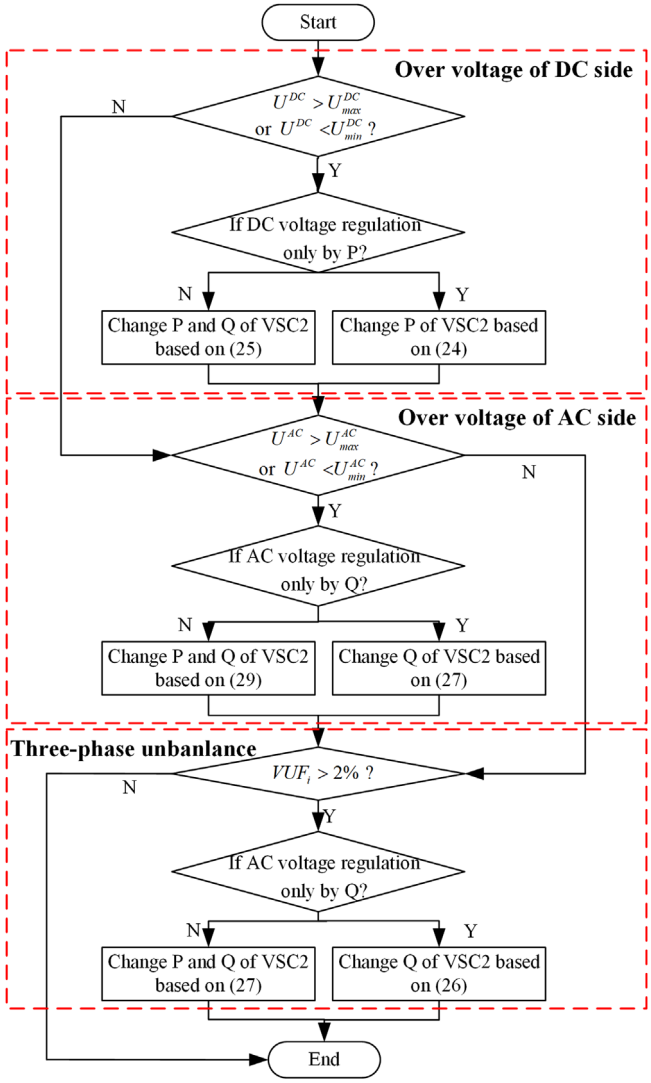

FIGURE 4 Flowchart of the proposed control strategy

by reducing the absolute value of the reactive power. At this time, VSC2's active and reactive power will be adjusted according to Equation (26).

$$\begin{cases} \sum \Delta P_{VSC2}^{AC,\varphi} = \Delta P_{VSC2}^{DC} \\ \left(P_{VSC2}^{DC} + \Delta P_{VSC2}^{DC}\right)^2 + \left(Q_{VSC2}^{AC} + \sum \Delta Q_{VSC2}^{AC,\varphi}\right)^2 = \left(S_{VSC2,\max}\right)^2 \end{cases}, \tag{26}$$

where $\sum \Delta P_{VSC2}^{AC,\varphi}$ and $\sum \Delta Q_{VSC2}^{AC,\varphi}$ are the sum of three-phase active and reactive power regulations on the AC side. As the active power regulation on the DC and AC sides should meet Equation (26), the voltage on the AC side will be affected when the active power regulation of VSC2 on the DC side changes. Therefore, there will be two solutions for Equation (26), in order to reduce the impact of the reactive power regulation on the AC side voltage, the solution with the smaller $\Delta Q_{VSC2}^{AC,\varphi}$ will be used. The relationship between single-phase voltage and the three-phase four-wire sensitivity of VSC2 should meet:

$$\Delta \mathbf{U}_{\mathbf{j}}^{\mathbf{AC}} = \mathbf{SAC}_{\mathbf{VSC2,j}}^{\mathbf{U-P}} \cdot \Delta \mathbf{P}_{\mathbf{VSC2}}^{\mathbf{AC}} + \mathbf{SAC}_{\mathbf{VSC2,j}}^{\mathbf{U-Q}} \cdot \Delta \mathbf{Q}_{\mathbf{VSC2}}^{\mathbf{AC}}, \tag{27}$$

where $\Delta \mathbf{U}_{\mathbf{j}}^{\mathbf{AC}}$ is the voltage deviation of node *j*. $\mathbf{SAC}_{\mathbf{VSC2,j}}^{\mathbf{U-P}}$ and $\mathbf{SAC}_{\mathbf{VSC2,j}}^{\mathbf{U-Q}}$ are the active-voltage and reactive-voltage sensitivity matrices of VSC2 and node *j*, the size of this two matrices is 4×4. $\Delta \mathbf{P}_{\mathbf{VSC2}}^{\mathbf{AC}}$ and $\Delta \mathbf{Q}_{\mathbf{VSC2}}^{\mathbf{AC}}$ are the active and reactive power adjustment matrices of VSC2 on AC side, the size of the two matrices is 4×1. It should be noted that the adjustable values of the active and reactive power of the neutral line of VSC2 are set to zero in order to meet the matrix dimension requirement. It is because that only the power of phase *a*, *b* and *c* can be adjusted of VSC2 while the sensitivity matrix is a fourth-order matrix.

If an AC node voltage exceeds the limits, the reactive power of VSC2 is firstly considered to regulate the voltage. This is because the DC line is not affected by the reactive power regulation on the AC side. The three-phase adjustment of reactive power of VSC2 on AC side can be preliminarily calculated by Equation (28).

$$\begin{bmatrix} \Delta Q_{VSC2}^{AC,a} \\ \Delta Q_{VSC2}^{AC,b} \\ \Delta Q_{VSC2}^{AC,c} \\ 0 \end{bmatrix} = \left[SAC_{VSC2,j}^{U-Q}\right]^{-1} \begin{bmatrix} \Delta U_j^{AC,a} \\ \Delta U_j^{AC,b} \\ \Delta U_j^{AC,c} \\ \Delta U_j^{AC,n} \end{bmatrix}, \tag{28}$$

$$\left[SAC_{VSC2,j}^{U-Q}\right] = \begin{bmatrix} SAC_{aa} & SAC_{ab} & SAC_{ac} & SAC_{an} \\ SAC_{ba} & SAC_{bb} & SAC_{bc} & SAC_{bn} \\ SAC_{ca} & SAC_{cb} & SAC_{cc} & SAC_{cn} \\ SAC_{na} & SAC_{nb} & SAC_{nc} & SAC_{nn} \end{bmatrix}, \tag{29}$$

where $\Delta U_j^{AC,\varphi}$ is the voltage deviation between the φ-phase voltage of node *i* and the upper or lower voltage limits. The upper and lower limits of the AC side voltage are taken as 1.07 p.u. and 0.90 p.u.

The over-voltage problems of any single-phase or multi-phase in AC lines can be addressed properly through coordinating the reactive power of phases *a*, *b* and *c* of VSC2 on the AC side when the active capacity is sufficient. Not only the three-phase adjustment value ($\Delta Q_{VSC2}^{AC,a}$, $\Delta Q_{VSC2}^{AC,b}$, $\Delta Q_{VSC2}^{AC,c}$) of VSC2 but also the corresponding influence on the neutral line's voltage ($\Delta U_i^{AC,n}$) of the power regulation can be obtained when the voltage exceeds the limit through solving Equation (28).

If the reactive capacity is insufficient when alleviating the AC side over-voltage, both active and reactive power will be used to coordinated regulate node voltages:

$$\begin{cases} \Delta U_j^{AC,\varphi} = \left[SAC_{VSC2,j}^{U-P}\right]_{rx} \cdot \left[\Delta P_{VSC2}^{AC,\varphi}\right] + \left[SAC_{VSC2,j}^{U-Q}\right]_{rx} \cdot \left[\Delta Q_{VSC2}^{AC,\varphi}\right] \\ \left(P_{VSC2}^{AC} + \sum \Delta P_{VSC2}^{AC,\varphi}\right)^2 + \left(Q_{VSC2}^{AC} + \sum \Delta Q_{VSC2}^{AC,\varphi}\right)^2 = \left(S_{\max}^{VSC2}\right)^2 \end{cases}. \tag{30}$$

The active power regulation of VSC2 on the DC side will change accordingly when the active power regulation on the AC side changes. However, the reactive power regulation of VSC2 on the AC side has no influence on the DC side. In order to reduce the active power regulation effect on the DC voltage, the active power adjustment value should be as small as possible. The magnitude of the active power decreases gradually in the calculation process of Equation (30). $\Delta Q_{VSC2}^{AC,c}$ will take the maximum value that meets the VSC2 capacity constraint until the voltage meets the constraint within 0.9 p.u. to 1.07 p.u.

(b) elimination of the three-phase unbalance

The VUF of the LVDNs is defined as follows:

$$VUF_i = \left(\frac{\max V_{i,\varphi} - V_i^{avr}}{V_i^{\text{avr}}}\right) \times 100\%, \tag{31}$$

where V_i^{avr} is the average voltage of three phase at node *i*:

$$V_i^{avr} = \frac{V_i^a + V_i^b + V_i^c}{3}. \tag{32}$$

The VUF_i should not exceed the 2% [29] when the network operation is normal. It should be noted that $\Delta U_j^{AC,\varphi}$ is the voltage deviation between the phase φ voltage and the average voltage of node *i*.

If a three-phase unbalance occurs on the AC side, considering the voltage margin under the distribution network regulation, the reactive power will be primarily adjusted according to Equation (28) to regulate the three-phase voltage to the average voltage of node *i*. If the reactive capacity is insufficient, Equation (30) will be used to achieve the coordinated control of active and reactive power so as to achieve three-phase voltage balance.

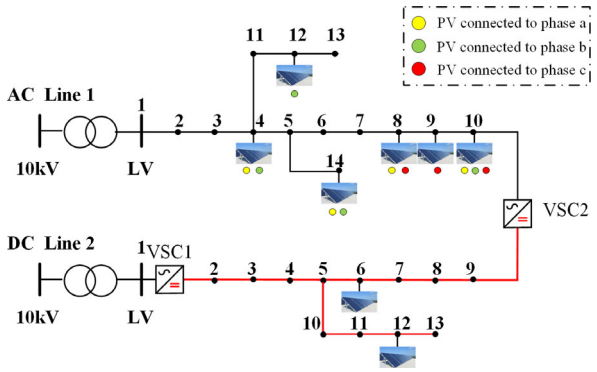

FIGURE 5 Test hybrid AC/DC LVDN

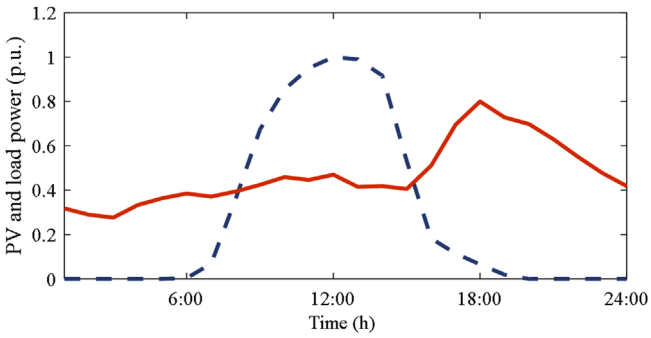

FIGURE 6 Power curves of PVs and loads

The flowchart of the proposed voltage control strategy is shown in Figure 4. The results of DC side over voltage processing that have already been done have not been affected when adjusting the active and reactive power of the VSC2, because the influence of power losses of VSC2 on the operation of the power system can be ignored.

4 | CASE STUDIES

Two case studies are conducted in this section. In Section 4.2, the sensitivity matrices are calculated, which is used to demonstrate the accuracy of the improved sensitivity matrix calculation method and the effect of voltage control based on the three-phase four-wire sensitivity on the AC side. In Section 4.3, a hybrid AC/DC LVDN is utilised to prove the effectiveness of the proposed control strategy on mitigating over-voltage and three-phase unbalance.

4.1 | Modelling of the hybrid AC/DC LVDN

A 27-node hybrid AC/DC LVDN is shown in Figure 5. There are two distribution transformers, a 13-node DC feeder and a 14-node AC feeder. The lines in the hybrid AC/DC LVDN are all overhead lines and the length of each section is 50 m. The line parameters and the three-phase loads connected of the AC side are shown in Tables A1 and A2. The resistance and admittance of each section of DC line are 0.65 Ω/km and 2.74×10^{-4} S/km, and the loads connected of the DC side are shown in Table A3. The position and the phases of the nodes of PVs are shown in Figure 5. The rated power of single-phase PV generation is 5 kW and the rated power of VSCs is 40 kVA. The 24-hour power curves of loads and PVs are shown in Figure 6. The voltage control interval of VSC2 is 1 h.

4.2 | Study 1: accuracy of proposed improved sensitivity calculation method

Perturb-and-observe' sensitivity calculation method [30] is used in Base case, and Equations (2) and (3) are used to calculate the self-sensitivities which do not consider the coupling effect and the influence from the neutral line in Case 1. Case 2 is the three-phase three-wire sensitivity calculation [31] without considering the neutral line effect. Case 3 is the three-phase four-wire sensitivity calculation method presented in this paper.

The power-voltage sensitivity matrices between VSC2 and node 8 on the AC side in different cases are shown in Table 1. As the smaller the disturbance ΔP and ΔQ the more accurate the sensitivity calculation results, the sensitivity matrices obtained in Base case are used as reference. The largest deviation of sensitivity is between Base case and Case 1. It is because the coupling effect and the influence from the neutral line on the sensitivity calculation is not considered in Case 1.

The maximum deviation in sensitivity calculations is 6.3 % and 12.7 % in Cases 3 and 2. That is because the neutral line has the influence on the other three-phase in sensitivity calculation in the unbalanced three-phase four-wire AC LVDNs. Moreover, the maximum deviation in sensitivity calculations between Base case and Case 3 is only 4.4 % on the DC side, as shown in Table 2.

Voltage control is performed based on the sensitivities calculated in Cases 2 and 3, respectively, in order to further verify the accuracy of proposed sensitivity calculation method.

DC line node voltages exceed the lower limit during 15:00–24:00, as shown in Figure 7(a). The sensitivities on the DC side will not be influenced by the sensitivity calculation methods in Cases 2 and 3, therefore the voltage control results on the DC side are the same.

As shown in Figure 7(b), the maximum voltage deviation on the AC side exceeds the upper limit during 8:00–18:00. During this period, the reverse power flow is formed in the line because of the high PV output and low load demand, which leads to the over-voltage issues. Moreover, the integration of single-phase grid-connection PVs and loads lead to the three-phase unbalance in the AC LVDNs.

The maximum voltages on the AC side are all within the requirement of 0.9 p.u. and 1.07 p.u. in Cases 2 and 3, as shown in Figure 7(c) and 7(d). However, the maximum VUF is 3.2 % in Case 2, while the maximum VUF is 0.95 % in Case 3, as shown in Table 3. Although the over-voltages are addressed in Cases 2 and 3, the VUF still exceeds the limit 2 % in Case 2. It is because when the same voltage deviation is adjusted, the power regulations (ΔP and ΔQ) in Case 2 are larger, and the voltage

TABLE 1 Active power-voltage sensitivity matrices between VSC2 and the node 8 on the AC side ($\times 10^{-4}$)

	Base case				Case 1	Case 2			Case 3			
Phase	**A**	**B**	**C**	**N**		**A**	**B**	**C**	**A**	**B**	**C**	**N**
A	16.9140	4.3810	5.0456	4.4002	11.8181	16.317	3.82632	4.96725	16.5470	4.10632	5.10725	4.4798
B	4.0985	16.294	3.1902	3.4112	11.5834	3.8208	16.372	0.9325	4.0508	16.6720	3.0725	3.4798
C	4.2082	5.2327	15.4112	3.3652	11.8274	3.875	4.80632	14.626	4.1050	5.10632	14.7660	3.4798
N	4.1112	3.2162	4.9551	15.4872	–	–	–	–	4.1050	3.10632	5.10725	14.9280

TABLE 2 Active power-voltage sensitivity matrices between VSC2 and the node 8–13 on the DC side ($\times 10^{-4}$)

Node	**8**	**9**	**10**	**11**	**12**	**13**
Base case	10.9035	14.3854	6.2877	6.3037	6.3088	7.0062
Case 3	10.4260	14.7422	6.4715	6.4793	6.4880	6.8858

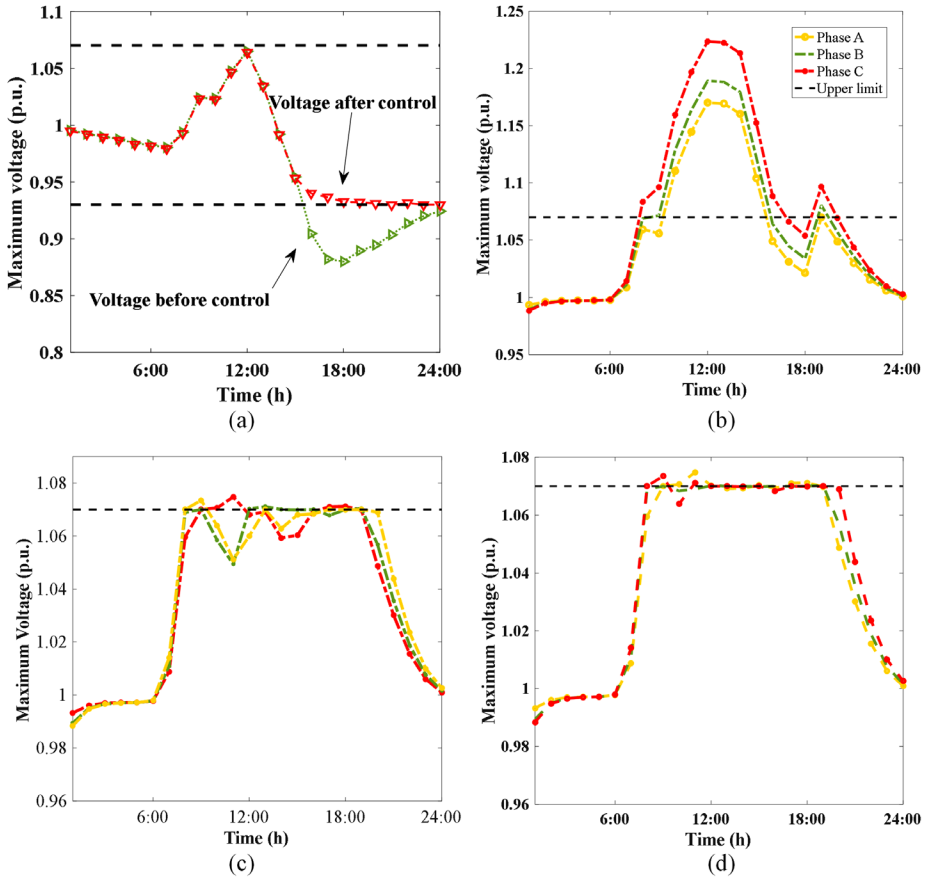

FIGURE 7 Maximum node voltages in the hybrid AC/DC LVDN. (a) Maximum voltage after control on the DC side; (b) Maximum voltage before control on the AC side; (c) Maximum voltage after control on the AC side in Case 2; (d) Maximum voltage after control on the AC side in Case 3

control capacity of VSC2 is insufficient when facing the three-phase unbalance problem.

Due to the interphase coupling and the influence of the neutral line in the three-phase four-wire line model, the position and phase of nodes are considered when calculating the sensitivity matrices in hybrid AC/DC LVDNs. Therefore, the three-phase four-wire sensitivity calculation method can achieve the highest accuracy. Moreover, the voltage control based on the

TABLE 3 Comparison of the voltage and VUF in 24 h

Solution method	Maximum voltage (p.u.)	VUF (%)
Case 2	1.0732	3.2
Case 3	1.0703	0.95

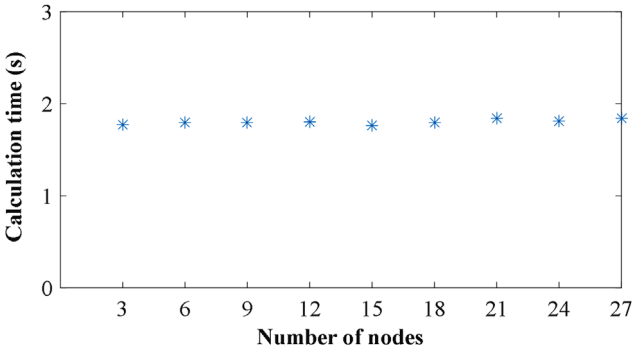

FIGURE 8 Three-phase four-wire sensitivity calculation time in Case 3

sensitivities calculated in Case 3 is most precise for the over-voltages and three-phase unbalance issues.

All tests are implemented using MATLAB R2016a on a computer with a 32-core AMD of 3.69 GHz and 64 GB memory. Figure 8 shows the calculation time curve of the proposed three-phase four-wire sensitivity calculation method in hybrid AC/DC LVDNs with different nodes. The sensitivity calculation time of a 27-node hybrid AC/DC LVDN used in this paper is 1.8386 s. The sensitivity matrices calculation time of 5-node, 9-node and 18-node hybrid AC/DC LVDNs is 1.7704 s, 1.7951 s and 1.7973 s. It can be observed in Figure 8 that the sensitivity calculation time is almost unchanged with the increase of the number of nodes in the hybrid AC/DC LVDNs. It is because the improved sensitivity calculation equations based on ABCD parameters are simple, which only relate to the line configuration and distribution network structure. The sensitivity calculation method presented in this paper not only improves the accuracy of the sensitivity matrices, but also greatly improves the calculation speed, because the three-phase four-wire sensitivities are calculated only by substituting line parameters (e.g. R and X) into the calculation formula.

4.3 | Study 2: superiority of proposed voltage control strategy of hybrid AC/DC LVDNs

In order to verify the effectiveness of the proposed control method, four cases are compared in this section. The Base Case has no additional control. In Case 1, only the ΔP and ΔQ are adjusted on the DC and AC side. Case 2 has the control strategy for the over-voltage and three-phase unbalance issues on the AC side. Case 3 uses the proposed control strategy for multiple issues in hybrid AC/DC LVDNs.

TABLE 4 Comparison of the voltage and VUF in 24 h

Solutionmethod	Maximum voltage of AC (p.u.)	VUF (%)	Minimum voltage of DC (p.u.)
Base case	1.2235	4.9	0.8800
Case 1	1.0747	3.4	0.9293
Case 2	1.0723	0.97	0.9293 (max voltage 1.094)
Case 3	1.0703	0.95	0.9300

In the Base Case, the three-phase voltages on the AC side have been over the upper limit from 8:00 to 18:00 and the VUF exceeds the limit during 9:00–15:00 due to the high penetration of PVs. The maximum over-voltage and VUF of AC side are 1.22 p.u. and 4.9 % as shown in Table 4. Under-voltage occurs on the DC side during 15:00–20:00 because of heavy loads. Maximum voltage deviation of DC is 0.83 p.u., as shown in Figure 9(a).

In the Case 1, although the voltage control of the VSC2 addresses the AC side over-voltage and the DC side under-voltage as shown in Figure 9(b), the maximum VUF (3.4% on the AC side) still exceeds the limit of 2%. This is because the reactive power adjusted of VSC2 to alleviate the three-phase unbalance is insufficient without fully considering the coordination of active and reactive power to realease VSC2's reactive power capacity on the AC side.

In the Case 2, the voltage deviation and the VUF are greatly reduced on the AC side, the maximum VUF is only 0.97 % and all the voltages are within the limit of AC. However, this strategy worsens the DC voltage, resulting in the original normal voltage exceeding the upper limit during 12:00–13:00, as shown in Figure 9(c). To mitigate the over-voltage and three-phase unbalance, the active power of VSC2 needs to be injected from DC side into AC side is 31 kW. However, the maximum transmission capacity of the DC side is only 25 kW. Therefore, node over-voltage of the DC side will occur after all the required power being absorbed from DC side without considering the constraint of DC load flow.

Figure 9(d) illustrates the voltages in the hybrid AC/DC LVDN with the control strategy proposed in this paper. The voltages always meet the voltage constraint on both AC and DC sides and the maximum VUF of AC is only 0.95%. With the proposed control strategy, the three-phase active power of VSC2 is absorbed from the AC side to mitigate the under-voltage on the AC side. Moreover, the coordinated control of the three-phase active and reactive power of VSC2 is achieved to improve the over-voltages and three-phase unbalances.

The control strategies in Cases 1 and 2 cannot address the issues simultaneously and completely neglecting the constraints of VSC capacity and DC power flow. The proposed strategy can realise a comprehensive improvement of voltage violations and three-phase unbalance issues.

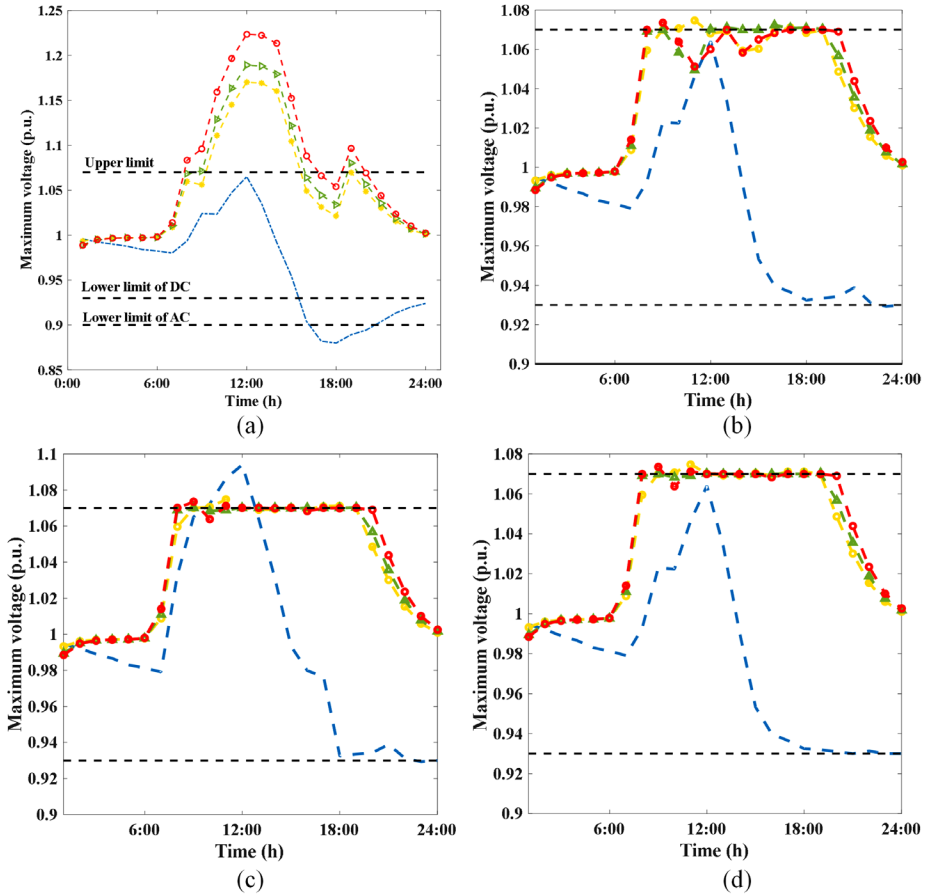

FIGURE 9 Maximum node voltages in the hybrid AC/DC LVDN. (a) Base Case; (b) Case 1; (c) Case 2; (d) Case 3

5 | CONCLUSION

This paper proposes an improved sensitivity calculation method for hybrid AC/DC LVDNs. The accuracy and effectiveness of the proposed voltage control strategy based on the improved sensitivity matrices on mitigating over-voltages and three-phase unbalance issues are analysed and demonstrated. Contributions include the improved sensitivity method considering three-phase four-wire grid structure and the position and phase of the nodes based on the ABCD parameters of the lines for hybrid AC/DC LVDNs, the coordinated control method including three-phase reactive power and active power of VSC considering the simultaneously happening of over-voltage and the three-phase unbalance in hybrid AC/DC LVDNs.

The proposed method has been verified through simulations. The results show that the improved sensitivity matrix calculation method can describe three-phase four-wire grid structure of AC side more accurately compared to the existing methods. Through the voltage control, the maximum voltage deviation and VUF on the AC side are all well regulated within the limits due to the precisely control by coordinating and controlling the three-phase power of VSC.

The voltage control method takes the advantages of the three-phase four-wire sensitivity and considers the constraints of VSC and DC power flow, which can address the power quality problems effectively in hybrid AC/DC LVDNs.

ACKNOWLEDGEMENT

This work was supported by The National Key Research and Development Program of China (2019YFE0118400).

CONFLICT OF INTEREST

The authors have no conflict of interest to disclose.

ORCID

Lu Zhang https://orcid.org/0000-0001-5696-2418
Chunxue Zhao https://orcid.org/0000-0002-8002-7558
Gen Li https://orcid.org/0000-0002-0649-9493

REFERENCES

1. Ntsaluba, S. B. K., Dlamini, I.: Performance and Cost analysis for a university based solar PV installation. Proceedings of the IEEE PES/IAS Power Africa, pp. 1-5 (2021)
2. Bai, F., Yan, R., Saha, T. K., et al.: An excessive tap operation evaluation approach for unbalanced distribution networks with high PV penetration. IEEE Trans. Sustain. Energy 12(1), 169–178 (2021)
3. Gutierrez-Lagos, L., Ochoa, L. F.: OPF-Based CVR operation in PV-rich MV–LV distribution networks. IEEE Trans. Power Syst. 34(4), 2778–2789 (2019)

4. Qiao, F., Ma, J.: Voltage/Var control for hybrid distribution networks using decomposition-based multiobjective evolutionary algorithm. IEEE Access, 8, 12015–12025 (2020)
5. Cai, Y., Tang, W., Li, L., et al.: Multi-mode adaptive local reactive power control method based on PV inverters in low voltage distribution networks. IET Gener. Transm. Distrib. 14(4), 542–551 (2020)
6. Ji, H., Wang, C., Li, P., et al.: Robust operation of soft open points in active distribution networks with high penetration of photovoltaic integration. IEEE Trans. Sustain. Energy 10(1), 280–289 (2019)
7. Li, P., Ji, H., Wang, C., et al.: Optimal operation of soft open points in active distribution networks under three-phase unbalanced conditions. IEEE Trans. Smart Grid 10(1), 380–391 (2019)
8. Liao, J., Zhou, N., Huang, Y., et al.: Unbalanced voltage suppression in a bipolar DC distribution network based on DC electric springs. IEEE Trans. Smart Grid 11(2), 1667–1678 (2020)
9. Zhang, S., Pei, W., Yang, Y., et al.: Calculation and analysis of total supply capability of AC/DC hybrid distribution network considering load balance. Proceedings of the 23rd International Conference on Electrical Machines and Systems, pp. 320–324 (2020).
10. Y, L., Yan, J., Han, X., et al.: Study on application of DC low voltage distribution system in rural area. Distrib. Util. 38(01), 17–24 (2021) (in Chinese)
11. Li, W., Li, Y., Yu, S., et al.: State of the art of researches and applications of MVDC distribution systems in power grid. Proceedings of the IECON 2019 - 45th Annual Conference of the IEEE Industrial Electronics Society, pp. 5680–5685 (2019)
12. Wu, T., Sun, K., Kuo, C., et al.: Predictive current controlled 5-kW single-phase bidirectional inverter with wide inductance variation for DC-microgrid applications. IEEE Trans. Power Electron 25(12), 3076–3084 (2010)
13. Huang, Y.: Day-Ahead optimal control of PEV battery storage devices taking into account the voltage regulation of the residential power grid. IEEE Trans. Power Syst. 34(6), 4154–4167 (2019)
14. Wick, S., Driessen, J.: Optimal local Reactive Power Control by PV Inverters. IEEE Trans. Sustain. Energy 7(4), 1624–1633 (2016)
15. Wang, P., Liang, D. H., Yi, J., et al.: Integrating electrical energy storage into coordinated voltage control schemes for distribution networks. IEEE Trans. Smart Grid 5(2), 1018–1032 (2014)
16. Zarate, M., Olshan, M. E. H., Guerrero, J. M.: Voltage quality improvement in low voltage distribution networks using reactive power capability of single-phase PV inverters. IEEE Trans. Smart Grid 10(5), 5057–5065 (2019)
17. Agalgaonkar, Y. P., Pal, B. C., Jabr, R. A.: Distribution voltage control considering the impact of PV generation on tap changers and autonomous regulators. IEEE Trans. Power Syst. 29(1), 182–192 (2014)
18. Jabr, R. A., Daric, I.: Sensitivity-based discrete coordinate-descent for Volt/Var control in distribution networks. IEEE Trans. Power Syst. 31(6), 4670–4678 (2016)
19. Meena, N. K., Yang, J., Singh, P.: Backward/Forward method for three-phase power flow calculation in low voltage distribution networks with EV charging points. Proceedings of the 2018 8th IEEE India International Conference on Power Electronics (IICPE), pp. 1–6 (2018)
20. Christakou, K., LeBoudec, J., Paolone, M., et al.: Efficient computation of sensitivity coefficients of node voltages and line currents in unbalanced radial electrical distribution networks. IEEE Trans. Smart Grid 4(2), 741–750 (2013)
21. Qiao, F., Ma, J.: Coordinated voltage/var control in a hybrid AC/DC distribution network. IET Gener. Transm. Distrib. 14(11), 2129–2137 (2020)
22. Jia, H., Xiao, Q., He, J.: An improved grid current and DC capacitor voltage balancing method for three-terminal hybrid AC/DC microgrid. IEEE Trans. Smart Grid 10(6), 5876–5888 (2019)
23. Fu, Y., Zhang, Z., Li, Z., et al.: Energy management for hybrid AC/DC distribution system with microgrid clusters using non-cooperative game theory and robust optimization. IEEE Trans. Smart Grid 11(2), 1510–1525 (2020)
24. Li, S., Yan, Y., Yuan, X.: SISO equivalent of MIMO VSC-Dominated power systems for voltage amplitude and phase dynamic analyses in current control timescale. IEEE Trans. Energy Convers. 34(3), 1454–1465 (2019)
25. Zheng, C., Zhou, X., Li, R., et al.: Study on the steady characteristic and algorithm of power flow for VSC-HVDC. Proc. CSEE 25(6), 1–5 (2005)
26. Lei, J., An, T., Du, Z., Yuan, Z.: A general unified AC/DC power flow algorithm with MTDC. IEEE Trans. Power Syst. 32(4), 2837–2846 (2016)
27. Liang, H., et al.: Study of power flow algorithm of AC/DC distribution system including VSC-MTDC. Energies 8(8), 8391–8405 (2015)
28. Cao, W., Wu, J., Jenkins, N., et al.: Benefits analysis of Soft Open Points for electrical distribution network operation. Appl. Energy 165, 36-47 (2016)
29. O'Connell, A., Keane, A.: Volt–var curves for photovoltaic inverters in distribution systems. IET Gener. Transm. Distrib. 11(3), 730–739 (2017)
30. Tamp, F., Ciufo, P.: A sensitivity analysis toolkit for the simplification of MV distribution network voltage management. IEEE Trans. Smart Grid 5(2), 559–568 (2014)
31. Youssef, K. H.: A new method for online sensitivity-based distributed voltage control and short circuit analysis of unbalanced distribution feeders. IEEE Trans. Smart Grid 6(3), 1253–1260 (2015)

How to cite this article: Zhang, L., Zhao, C., Zhang, B., et al.: Voltage control method based on three-phase four-wire sensitivity for hybrid AC/DC low-voltage distribution networks with high-penetration PVs. IET Renew. Power Gener. 1–13. (2021) https://doi.org/10.1049/rpg2.12350.

APPENDIX A

The derivation process of Equation (2) is as follows. The derivation process of Equation (3) is similar.

The voltage of any node j in the distribution network is expressed as

$$U_j = U_i - \sum_{l \in C_{i,j}} \frac{P_{\text{line},l} R_l + Q_{\text{line},l} X_l}{U_l}. \tag{A.1}$$

where $P_{\text{line},l}$ and $Q_{\text{line},l}$ are the active power and reactive power of the distribution line between nodes l-1 and l. R_l and X_l are the equivalent resistance and reactance of the distribution line between nodes l-1 and l.

The transmission power of the distribution line meets the relationship:

$$\begin{cases} P_{\text{line},l} = \sum_{k=l}^{n} P_{\text{load},k} + \sum_{k=l+1}^{n} P_{\text{loss},k} \\ Q_{\text{line},l} = \sum_{k=l}^{n} Q_{\text{load},k} + \sum_{k=l+1}^{n} Q_{\text{loss},k} \end{cases}, \tag{A.2}$$

where $P_{\text{load},k}$ and $Q_{\text{load},k}$ are the active power and reactive power of the load connected to the node k. $P_{\text{loss},k}$ and $Q_{\text{loss},k}$ are the active and reactive power losses of the line between nodes k-1 and k.

The power losses of the line are ignored to simplify the derivation result, because they are small in proportion to the

TABLE A1 The impedance and admittance of the AC LVDNs

Phase	Impedance (Ω/km)				Admittance (S/km)
	A	B	C	N	
A	0.6500 + j0.41200	0.0065 + j0.00412	0.0065 + j0.00412	0.0065 + j0.00412	2.74×10^{-4}
B	0.0065 + j0.00412	0.6500 + j0.41200	0.0065 + j0.00412	0.0065 + j0.00412	2.74×10^{-4}
C	0.0065 + j0.00412	0.0065 + j0.00412	0.6500 + j0.41200	0.0065 + j0.00412	2.74×10^{-4}
N	0.0065 + j0.00412	0.0065 + j0.00412	0.0065 + j0.00412	0.6500 + j0.41200	2.74×10^{-4}

TABLE A2 Loads on the AC LVDNs (kW)

Phase	Node						
	1	2	3	4	5	6	7
A	2.0040 + j0.8020	1.7870 + j0.7150	1.5460 + j0.6180	1.3520 + j0.5410	0	3.2840 + j1.3140	0
B	0.9450 + j0.3780	2.3520 + j0.9410	1.3020 + j0.5210	1.7640 + j0.7060	1.4505 + j0.5820	4.0320 + j1.6130	2.5410 + j1.0160
C	1.6400 + j0.6560	1.440 + j0.5760	1.7000 + j0.6800	2.3400 + j0.9360	2.9950 + j1.1980	2.9000 +j1.1600	2.9600 + j1.1840
Phase	**8**	**9**	**10**	**11**	**12**	**13**	**14**
A	0	4.6800 + j1.8720	2.1205 + j0.8500	0	2.0770 + j0.8310	2.0040 + j0.8020	1.7870 + j0.7150
B	2.5830 + j1.0330	1.4280 + j0.5710	0	2.3730 + j0.9490	1.4070 + j0.5630	0.9450 + j0.3780	2.3520 + j0.9410
C	3.1200+j1.2480	1.7000 + j0.6800	2.0305 + j0.8140	3.0000 + j1.2000	1.9600 + j0.7840	1.6400 + j0.6560	1.4400 + j0.5760

TABLE A3 Loads on the DC LVDNs (kW)

1	2	3	4	5	6	7	8	9	10	11	12	13
2.8350	7.0560	3.9060	5.2920	4.3650	12.0960	7.6230	7.7490	4.2840	3.7050	7.1190	4.2210	10.0200

total transmission power of the distribution line.

$$\begin{cases} P_{\text{line},l} \approx \sum_{k=l}^{n} P_{\text{load},k} \\ Q_{\text{line},l} \approx \sum_{k=l}^{n} Q_{\text{load},k} \end{cases}. \tag{A.3}$$

The active power-voltage sensitivities can be obtained by calculating the derivative of Equation (1) with respect to active power:

$$\begin{aligned} \frac{\partial U_j}{\partial P_i} &= \frac{\partial U_i}{\partial P_i} - \sum_{l \in C_{i,j}} \left(\frac{\partial}{\partial P_i} \left(\frac{P_{\text{line},l} R_l}{U_l} \right) + \frac{\partial}{\partial P_i} \left(\frac{Q_{\text{line},l} X_l}{U_l} \right) \right) \\ &= - \sum_{l \in C_{i,i}} \frac{\partial}{\partial P_i} \left(\frac{P_{\text{line},l} R_l}{U_l} \right) \approx - \sum_{l \in C_{i,i}} \frac{R_l}{U_l} \frac{\partial}{\partial P_i} \sum_{k=l}^{n} P_{\text{load},k} \end{aligned}. \tag{A.4}$$

The result of analysis of the derivative elements in the above equation is

$$\frac{\partial P_{\text{load},k}}{\partial P_i} = \begin{cases} 1, \text{if } k = i \\ 0, \text{if } k \neq i \end{cases}. \tag{A.5}$$

Equation (A.6) can be obtained by substituting the Equation (A.5) into Equation (A.4):

$$S_{j,i}^{U-P} = \frac{\partial U_j}{\partial P_i} \approx - \sum_{l \in (C_{0,i} \cap C_{0,j})} \frac{R_l}{U_l}, \tag{A.6}$$

where $S_{i,j}^{UP}$ is the active power-voltage sensitivity. $C_{0,i} \cap C_{0,j}$ represents the intersection set of the two sets of lines.